Breaking up and making up – reworking of Holocene calcarenite platform into rapidly-forming beachrock breccias on a high energy coastline (St. Lucia, South Africa)

Falkenroth, M., Green, A. N., Cooper, A., Menzel, M., & Hoffmann, G. (2021). Breaking up and making up – reworking of Holocene calcarenite platform into rapidly-forming beachrock breccias on a high energy coastline (St. Lucia, South Africa). *Sedimentology*, *69*(3), 1339-1364. https://doi.org/10.1111/sed.12953

Published in:
Sedimentology

Publication Status:
Published (in print/issue): 27/10/2021

DOI:
10.1111/sed.12953

Document Version
Peer reviewed version

Breaking up and making up – reworking of Holocene calcarenite platform into rapidly-forming beachrock breccia on a high energy coastline (St. Lucia, South Africa)

Falkenroth, M.[1,2]*; Green, A.N.[3]; Cooper, J.A.G.[3,4]; Menzel, M.[5]; Hoffmann, G.[2]

[1] NUG, RWTH Aachen University, Aachen, Germany
[2] Environmental Geology, Institute of Geoscience, University Bonn, Bonn, Germany
[3] Geological Sciences, University of KwaZulu-Natal, Durban, South Africa
[4] School of Environmental Science, University of Ulster, Antrim, United Kingdom
[5]GED, RWTH Aachen University, Aachen, Germany

*Corresponding Author

Keywords: Beachrock, South Africa, Coastal Geology, Geomorphology, Holocene, Sea-Level, Facies Analysis

Abstract
Beachrocks are a common characteristic of tropical and subtropical coastlines. It is known that they have a substantial influence on beach morphodynamics and they are often utilised as indicators of palaeo sea levels. At the same time facies variability in beachrocks is understudied and their effect on shoreline evolution is poorly understood. At Mission Rocks on the KwaZulu-Natal coastline of South Africa a narrow beach with isolated sand patches occupies low points of an otherwise continuous 3 m-thick, raised shore platform of sandy and gravelly beachrocks. These beachrocks are in the process of disintegrating into megagravel deposits through chemical and mechanical weathering in a wave-dominated, high-energy setting. The breakdown is potentially slowed by a contemporary, fast-forming beachrock facies, that blankets the surface and fills fractures and potholes within the older platform. The accumulation and cementation of this recent beachrock is the focus of this study. The beachrock is dated by historical evidence to post-WWII. Data from field observations, petrographic and geochemical methods, reveal that the cementing agents of the beachrock were precipitated from marine water in a phreatic setting despite its position above the intertidal. Not only does this facies have implications for the interpretation of paleo beachrock as a sea level indicator, it also raises further questions regarding modelling of coastal erosion of beaches associated with outcrops of beachrock.

1. Introduction
Beachrocks are bodies of cemented beach sediments, that form in situ within the beach system. They are found on coastlines worldwide, although the vast majority of occurrences are located between latitudes of 20° and 40° (Vousdoukas et al. 2007a). Only a few reports of beachrocks in temperate or colder climates exist (e.g. Binkley et al. 1980, Rey et al. 2004, Kneale and Viles 2000, Cooper et al. 2017). The cement that binds the sediment together is usually calcium carbonate, either aragonite or calcite, whereby calcite appears as a low-magnesium (LMC) and a high-magnesium (HMC) variation (Bricker 1971, Stoddart and Cann 1965). A variety of processes are responsible for beachrock

cementation, those are: precipitation from seawater (Ginsburg 1953), $CaCO_3$ flux as a response to mixing of marine and meteoric waters (Milliman 1974), evaporation of groundwater in arid settings (Russell and McIntire 1965), CO_2 degassing from dissolved $CaCO_3$-rich groundwater (Hanor 1978) and microbial activity (Neumeier 1999). The timescale on which beachrock-formation takes place varies considerably (Hopley 1986). While it was suspected early on that cementation can take place rapidly, studies that provided proof in the form of well constrained ages of young beachrocks were rare. Several studies document how fast beachrock formation can occur (Frankel 1968, Easton 1974, Chivas et al. 1986, Cawthra & Uken 2012, Vousdoukas et al. 2007a, Wiles et al. 2018), but there is still an overall dearth of studies in this regard. With this study we contribute further examples of very young beachrocks, based on historical evidence that indicates a depositional age postdating 1943.

Given a particularly rapid cementation process, beachrocks have a proclivity to act as good archives of paleo-environmental information via the snapshot preservation of their sedimentological facies. Through rapid lithification, a beachrock holds all the sedimentological structures, traces of biological activity and sediment characteristics of the beach section, in which it initially formed. Therefore a sedimentological facies analysis can help reconstruct coastal parameters like sediment influx, energy level, ecosystem changes, sea-level variations and extreme wave events (Kelly et al. 2014). The cementation process also causes beachrocks to be resistant to erosion, which is why they effectively preserve information of paleo-shorelines over geological timescales (e.g. Yaltirak et al 2002, Calvet et al. 2003, Falkenroth et al. 2019) as compared with only shorter term observations based on coastal dynamics or stratigraphy of unconsolidated sediments. It is widely acknowledged that beachrock lithofacies are highly variable (Kelly et al. 2014); their interpretation together with the cementation phases is thus useful when using beachrock as a sea-level indicator (Vacchi et al. 2012, Mauz et al. 2015) or when studying shoreline evolution with the aim to make assumptions on future shoreline developments (Cooper 1991(a)). However, the facies variability of beachrocks remains understudied. Beachrocks are almost exclusively described as seaward dipping, slab-shaped, low energy sediments on dissipative beach profiles (e.g. Russel 1959, Davies and Kinsey 1973, Moore 1973, Badyukova and Svitoch 1986).

Our knowledge about facies variability, preservation potential, geological inheritance in beachrocks, and how changes in shoreline morphology can be accordingly tracked is surprisingly incomplete. In this study we aim to contribute to what is known about beachrock facies variability. This paper examines a contemporary beachrock facies on a high energy coastline, that has resulted from the simultaneous breakdown of an older beachrock platform. The facies is unique in that it plays a dual role in the continuous cycle of erosional breakdown and simultaneous depositional build-up of a beachrock platform. This is a hitherto undescribed process which is neglected in models of rocky shoreline evolution. Likewise, the beachrock occurrence as a thin veneer that fills erosional hollows in a rocky platform structure is unique. This leads to further questions about its cementation process, considering that cementation is thought to occur below a significant overburden of sediment in the marine vadose-phreatic mixing zone (Hopley 1986, Mauz et al. 2015). The main purpose of this study is to unravel the formation process of the unusual beachrock facies at Mission Rocks and to consider the implications of its formation for shoreline stability.

2. Regional Setting

This study focuses on Mission Rocks, a mixed sand and rock shoreline that forms part of the iSimangaliso (Greater St. Lucia) Wetland Park (Fig. 1). The park is located on the east coast of South Africa, bordered by the Indian Ocean to seaward and a series of wetlands and coastal lake systems located to landward (Dladla et al. 2019). The area has a humid subtropical climate with a mean annual temperature of 21.6 °C (Maud, 1980) and an annual precipitation of 1100 mm, which decreases inland (Midgley et al., 1994). The coast is considered wave-dominated, with a mean significant wave height

(H_S) of 1.8 m (Moes and Roussouw 2008). The spring tidal range of 1.84 m, with a maximum tidal height of 2.47 m (Smith et al. 2010), categorises the coastline as upper microtidal to low mesotidal (cf. Hayes 1979).

The region is underlain by Cretaceous age siltstones of the St Lucia Formation. Some isolated outcrop is found to the northwest, at Listers Point (Cooper et al. 2013), however this mostly occurs in subcrop to the coast. The only other rocky outcrop found comprises beachrocks and aeolianites (Coetzee, 1975). The rivers that debouch to the area drain a variegated catchment geology that comprise Archaean-age granites, quartzites, phyllites, greenstones and occasional banded ironstones of the Pongola Supergoup (Hicks 2009), some Proterozoic gneisses of Tugela terrain (McCourt et al. 2006), and Jurassic age dolerites (Hastie 2012) are also intersected. Approximately 100 km to the south, outcrops of Late Carboniferous-Early Permian Dwyka Formation diamictites and Permian age Vryheid Formation sandstones and shales are found.

The coastline is dominated by a series of long, linear beaches that are bordered to landward by well-vegetated, up to 180 m high dunes (Porat and Botha 2008). These dunes are locally disrupted by outlets of coastal lagoons and river estuaries (Ramsay 1994). During the Last Glacial Maximum (LGM), sea-level was 100 to 130 m below the present level (Cooper et al. 2018), which led to the subaerial exposure of the adjoining shelf (Green 2009). Several river valleys incised the main dune cordon to the north and south of the study area (Benallack et al. 2016; Dladla et al. 2019). With the ensuing transgression of the Holocene, these later formed sites for inlets in the then stabilised Holocene shoreline that had formed against the pre-existing mainland dunes (Cooper 1991(b)). This transgression submerged a number of aeolianites and beachrocks on the shelf, observed as coast parallel ridges in the region (Salzmann et al. 2013). Holocene sea levels reached the present day elevation ~ 7000 cal BP, before rising to a Holocene highstand of +3.8 m between 6500 and 5500 cal BP (Cooper et al. 2018). The highstand is correlated with a variety of raised beachrocks that span the coastline from Durban (Cooper and Green 2016) to the Mozambique border (Ramsay 1995).

The Mission Rocks coast comprises isolated sand patches that occur in low points of an otherwise continuous 3 m-thick raised shore platform of sandy and gravelly beachrocks. These beachrocks were first described as aeolian deposits and beachrocks by Coetzee (1975), who linked their cementation to the recent late Holocene sea-level stillstand. Cooper (1991(b)) ascribed their thickness to the inhibited landward migration of the Holocene shoreline, thus allowing several generations of beachrock to superimpose one another. The high energetic regime of the coastline has led to erosion of the beachrock, whose products partly cover the beach in form of clustered megagravel deposits (Salzmann and Green 2012).

In the early 1940s, the raised shore platform was dynamited and quarried for materials used in the construction of a base for the flying planes (Catalinas) that operated out of the adjoining lake system at Lake St Lucia (Fig. 1). Several large, radially-oriented fractures are still evident from the quarrying process (Fig. 2). These can be dated to a maximum age of 1943 (Gaisford 2011).

3. Methods

A 1.3 km stretch of the raised shore platform at Mission Rocks was mapped for variation in beachrock facies. All coordinates are presented as latitude and longitude and are used to mark significant occurrences in such beachrock facies. The facies and spatial relationship of the beachrock with the underlaying calcarenites were described and photographed.

Site elevations are derived from a terrestrial Lidar survey flown in 2016 at an elevation of ~ 1050 m. A vertical accuracy of ~ 10 cm in the z domain was achieved, with an average density of 1.5 points per square meter. The data are presented as ground strikes and are related to multiple ground control points. The digital elevation model (DEM) derived from the LIDAR data has a pixel spacing of 0.1 m.

All samples were analysed from standard thin sections (2 cm wide, 5 cm long and 25 µm thick) using a polarising microscope (Leica DMEP). Transmitted light microscopy was used for cement identification and phase type, in addition to compositional variability. One thousand points were counted in the cement of each thin section along evenly spaced traverses to determine the volume share of each cement type.

In order to analyse the morphology of the cement crystals, Scanning Electron Microscope (SEM) images were taken with a Zeiss Gemini SUPRA 55 field-emission electron microscope. The SEM is coupled to an automated energy-dispersive X-ray spectrometer (EDS), which was used to acquire point EDS spectra of the cements on non-polished samples of the material. The samples were coated by a 6 – 8 nm thick layer of tungsten to heighten conductivity.

The SEM images were obtained at high vacuum employing an acceleration voltage of 3 KV and a 8.6-11.2 mm working distance. Different magnifications (between 82x and 13450x) were used to take images by a secondary electron detector. The elemental analysis was carried out using an 8.6 mm working distance and an acceleration voltage of 16 KV.

4. Observations

An usual beachrock facies occurs at least at six locations on Mission Rocks beach as infill of potholes, factures and erosional gullies within or blanketed over the surface of older calcarenites (see Fig. 1). The occurrences of this facies lies between 1.08 m and 1.96 m above mean sea level (msl) and thereby above the intertidal zone as measured by the mean spring tidal range of 1.84 m. However, the high energy level of the coastline with a mean annual wave height of 1.8 m, causes a significant amount of spray that is applied almost constantly. For an overview of all observations see Table 1.

4.1. Macrofacies

This beachrock facies comprises a very poorly sorted, polymictic, clast-supported breccia (see Fig. 3: I and IV). The framework clast sizes range from very small pebbles to small boulders of up to 40 cm in diameter. A medium sand to granule sized matrix is notable. The ratio of matrix to larger clasts varies, where the facies occurs as infill in narrow fractures, the material is often clast supported. Generally, this matrix has a similar composition to the contemporary beach sand at Mission Rocks. At outcrops E and F, the matrix consists of heavy minerals (mostly garnets), which give it a dark red to purple colour (see Fig. 3: III). The fabric of the sediment is chaotic, no primary orientation of clasts is visible, however a significant portion of disc- or rod-shaped clasts are found cemented in an upright position (i.e. Fig. 3: II and IV). No sedimentary structures are evident.

Two different kinds of clasts can be recognized. The first are exotics derived from geology of the hinterland and only found in association with the catchment geology of the adjoining fluvial systems. These include granite, shale, dolerite, quartzite, banded iron formation, greenstone, diamictite and non-calcareous sandstones, none of which crop out in close proximity to the study site or can be found among the recent beach sediment. These clasts make up roughly 35% of the entire clast content, are well rounded and not larger than small cobble size. The second clast types comprise intraclasts that were quarried from the underlying beachrock platform. These clasts make up the larger share of 55%, are particularly angular and occur mostly as cobble to boulder sized clasts.

The clasts are also fossiliferous with mostly bivalve- and gastropod-shell debris. Most shells are heavily disaggregated (and thus beyond taxon identification), with only oysters (Crassostrea sp) and black mussels (Perna perna) identifiable. To seaward, the breccia becomes more shell-rich and shows an overall smaller clast size with an increased shelly matrix content.

4.2. Microfacies

The framework grains are usually quartz or lithic fragments, with lesser amounts of shell fragments, weathered olivine and opaque minerals. The sediment is cemented to a varying degree. While in samples 13 and 15 the primary porosity is almost completely filled by cementing agents, in sample 14 the cements occur as isopachous crusts and menisci, but are rarely pore-filling. The remaining porosity, if any, is mostly intergranular and only rarely intragranular (i.e. cavities within shells) as most fragile components that would provide such intragranular porosity are shattered.

4.2.1. High-Mg-Calcite Micrite Cements

Micrite occurs in all three samples as rims on grain surfaces, as meniscus or pore-filling cement (see Fig. 4: II) or as pseudo peloids. Pore-filling micrite is found in sample 14 (6.6% of cement volume) and sample 15 (27.8% of cement volume). It is very fine grained, with a black colour and no internal structure. Sample 13 shows a pore-filling pseudospar that comprises up 29.2% of the total cement volume. This exhibits a grainy texture with varying intensity, the pseudospar forming as a the result of recrystallisation of a former micritic porefilling. Micrite rims occur in all three samples and account for between 12.3% of total cement volume in sample 15 and 24.9% in sample 14. While the micrite rims are between 15 and 30 µm thick with a consistent rim thickness in sample 15 (see Fig. 4: I), they mostly vary in rim thicknesses, e.g. ranging between 10 and 100 µm as in sample 14 (see Fig. 4: IV). In sample 13 the majority of the micrite rims have recrystallised into pseudospar, leaving only a thin (10 to 15 µm), irregular layer of micrite on the surface of some grains.

The micrite rims are brownish/grey to black and cover either the surface of a grain directly or the surface of other crust cements, sometimes indicating several cycles of cementation (see Fig. 4: III). On most surfaces the border between micrite rim and grain is sharp, which indicates a constructive micritic rim (see Fig. 4: IV), but destructive micritic envelopes also occur (see Fig. 4: III). The latter are encountered rarely, because they are limited to carbonate grains and most of the clast content is siliciclastic. Micrite menisci are observed in all three samples and make up between 1.4% of total cement volume in sample 13 and 8.4% of cement volume in sample 15. The menisci exhibit a curved surface and are found at grain-to-grain contacts. Sample 13 is the only sample in which pseudo peloids are observed. These peloids range in diameter between 5 and 20 µm and show an irregular, elongated shape (see Fig. 4: V). They occur between the prismatic crystals of isopachous rims.

Scanning electron microscope (SEM) analyses show no internal structure of the micrite rims (see Fig. 5: II). However, very small (2 to 10 µm long) acicular crystals are found to form on the surface of micrite rims (see Fig. 5: I). Pore-filling micrite, meniscus micrite and pseudo peloids were only observed in plane light. Four EDX spectra were obtained from micrite rims, which show an average Mg-content of 85.6 mol-% in sample 15 and 27.5 mol-% in sample 14 (see Table 3).

4.2.2. High Mg-Calcite Crust Cements

Crust cements are common in all three samples and consist of either prismatic crystals, pseudospar or dog-tooth crystals. Fibrous rims of prismatic crystals that stand perpendicular to the grain surface are the most common style of cement in all three samples, making up between 41.6% of total cement volume in sample 13 and 31.2% in sample 15 (see Table 2). While they form irregular crusts that thicken towards the centre of the pores in sample 13, in samples 14 and 15 they form isopachous rims, with a very consistent thickness between 50 and 200 µm. In all samples they can fill the entire pore space. Up to seven individual cycles of cementation are found within some crusts (see Fig. 4: III). The first cycle typically produces the thickest layer of cement, the individual cycles are interrupted by thin layers of micrite. Occasionally at grain contacts or in narrow spaces between grains, the prismatic crystals can phase into a fine grained pseudospar (ps in Fig. 4). Dog-tooth crust cements are rarely encountered, they only comprise 1.1 volume% of cements in sample 14 (see Table 2). The individual crystals are sharply pointed, grow normal to the grain surface and reach a length of up to 20 µm (see Fig. 5. III). Ten EDX spectra were obtained from the prismatic crust cements. All of them show a high Mg-calcite composition between 17.5 mol-% Mg in sample 15 and 22 mol-% Mg in sample 14 (see Table 3).

4.2.3. Pore-filling Cements

These cements fill out entire pores without being bound to grain surfaces. Pore-filling cements occur as pseudospar, as drusy spar (see Fig. 4: I and fig. 4: V) and as equant spar. Pseudospar is the most common pore-filling cement, consisting of up to 29.2% of total cement volume in sample 13, 21.5% in sample 14 and 11% in sample 15. Equant, pore-filling spar is also encountered in all samples but is less common, only accounting for 7.9% in sample 13. In samples 14 and 15 equant spar is exclusively found within beachrock intraclasts and makes up 0.4% (sample 15) to 6.1% (sample 14) of total cement volume. Drusy spar occurs in samples 13 (4.5%) and 15 (8.4%). The pseudospar shows a grainy texture and a dark grey colour, it often phases gradually into micrite or larger crystals. Within beachrock intraclasts the equant spar forms epigranular, subhedral crystals that completely fill the pores and are up to 200 µm in diameter (see Fig. 5 IV). In sample 13 it forms at the centre of pores and grades into pseudospar towards the pore-edges. It displays anhedral crystal shapes and crystal sizes between 50 and 100 µm. The drusy cement occurs as void infill in samples 13 and 15 and consists of equant, anhedral calcite crystals, usually 10-20 µm in size.

One EDX spectrum was obtained from the pseudospar pore-filling in sample 13 – there it shows a Mg-content of 34 mol-%. The blocky, equant spar shows a low-Mg Calcite composition within the intraclasts in sample 15 and a high Mg-Calcite composition in sample 13 (see Table 3). Six of the EDX spectra obtained from drusy pore-filling cement in sample 13 show a high Mg-Calcite composition (average 18 mol-% Mg), while two from the same sample display a low Mg-Calcite composition (average 6 mol-% Mg). In sample 15 the drusy pore-filling cement also consists of low Mg-Calcite with an average of 1 mol-% Mg.

4.3. Spatial Relationship

The beachrock breccia is blankets portions of the surface of the calcarenite-platform at Mission Rocks. Most occurrences are located within weathering structures, such as potholes, fractures, or gullies. These structures function as accommodation space, provide shelter from erosion and, in some cases, contain tidal pools, which contribute to cement growth.

At outcrop A the breccia is found within a 0.3 m wide fracture between two in situ beachrock blocks (see Fig. 6A). At outcrop B the breccia fills a 0.28 m-deep, raised-rim pothole. Here the thickness of the breccia does not exceed 0.15 m (see Fig. 6B). At outcrop C the breccia is found at the base of an erosional gully (see Fig. 6C). Outcrop D is located on top of the older beachrock platform, with prominent, up to 1.5 m-deep fractures and potholes in which the beachrock breccia has formed (see Fig. 6D). The breccia covers the floor and the sidewalls of the potholes and has a highly irregular surface. At outcrop E the beachrock breccia occurs in patches or elongated rims on top of a flat beachrock platform in the backshore (see Fig. 6E). This outcrop is especially significant, since the surface on which the breccia has formed shows the remains of quarrying activity during the 1940s. The breccia fills the radial fractures and quarry slots within the quarried beachrock platform. On the northernmost end of the beachrock platform (outcrop F), the breccia drapes a heavily eroded surface, which shows *Spitzkarren* structures (see Fig. 6F). Here the breccia is at least 0.2 m thick.

5. Discussion

5.1. Age constraint

During WWII, the Holocene calcarenite platform of Mission Rocks beach was mined for building purposes (Gaisford 2011). This quarrying activity was carried out partly using explosives that left radial fractures in the platform, which are still visible today (see Fig. 2). At outcrop E the beachrock facies described in this study occurs covering these fractures, thus implying an age younger than the last mining activity in 1943 (see Fig. 3 I). Although it cannot be assumed that all occurrences of this unusual beachrock facies are of the same age, this still shows that this facies formed at least partially during the last 77 years. We consider that this rapid formation of new beachrock slows the disentegration rate of the underlying calcarenites especially since the formation takes place within gullys, fractures and potholes, thus counteracting the gravitational, chemical and mechanical breakdown of the beachrock platform (cf. Cooper et al. 2019).

5.2. The Formation of the Unusual Beachrock Facies

The development of the described beachrock involves two stages: (1) deposition of a beach on the landward side and on top the calcarenite platform and (2) cementation of the loose sediment.

(1) The deposition of sand and gravel at Mission Rocks is facilitated by the presence of the calcarenite platform. The platform generates accommodation space by sheltering its landward side from the continuously high wave action that occurs to seaward. Despite wave incursions over the platform (Salzmann and Green 2012; Green et al. 2018), the irregular topography (cracks, potholes, quarry slots) and elevated seaward edge of the platform capture and retain sediment.

The matrix of the beachrock shows a similar composition to the loose beach material, especially where this material fringes rocky outcrop. However, in the breccia, the portion of gravel-sized clasts is much higher. Within fractures and gullies of the calcarenite platform the beachrock can even be clast-supported. The accumulation of clasts within fractures is due to a sieving effect of the platform by wave action, with the angular clasts concentrating in the lowermost portions of the platform surface forming fitted textures predisposing them to preservation (cf. Reference). The movement of clasts within confined spaces also explains the upright position of some of them, i.e. rods or discs sliding into narrow openings. One notable exception is outcrop A, where disc-shaped clasts are found cemented in an upright position although not located within a confined space. This kind of fabric can only be achieved if a large body of sediment is rapidly deposited and no further reworking prior to cementation occurs. This indicates a sudden drop in energy level followed by rapid cementation. At outcrops A, C, D and E the beachrock contains a very high proportion of intraclasts derived from the underlying calcarenite platform. These intraclasts have undergone no significant transport or reworking by waves, as demonstrated by their large grainsize (mostly small boulders up to 0.5 m in diameter) and angular shape. See Fig. 7 for a visual representation of the beachrock formation.

(2) The cementation process of this beachrock is somewhat contradictory to the typical models of high magnesian calcite-forming cements (cf Mauz et al. 2015). These recent beachrocks are located within the spray zone in the meteoric vadose environment, however the cements are more indicative of the marine phreatic to marine vadose zones. In all three samples the largest share of cement (over 90% of total cement volume) consists of high magnesium calcite (HMC) in various forms. HMC is attributed to precipitation from marine waters, as meteoric water typically has a very low Mg/Ca ratio and thus constitutes the precipitation of low magnesium calcite (LMC) (Fluegel 2010). The first step of cementation in all samples is micrite or microscrystalline material either as pore-filling or circumgranular rims and menisci (see Fig. 6). Micrite precipitation was linked to microbial activity in several studies (Kobluk & Risk 1977, Calvet 1982, Wright 1986). While the formation of meniscus

cement is generally interpreted as indicative of the vadose zone (e.g. Mauz et al 2015, Fluegel 2010), Hillgärtner et al. (2001) show that meniscus micrite is not a good indicator of a vadose setting as its formation is linked to grain-binding by organic filaments and thus just as likely in phreatic environments. In this case, there are no other meniscus cements or gravitational structures that would indicate precipitation in the vadose zone.

Symmetrical, HMC, isopachous rims, as observed in samples 14 and 15, indicate pores that were filled completely with water in a marine phreatic setting. A minor meteoric influence is present in the form of LMC equant and drusy spars, that represent the last cycle of cementation and make up the smallest share of total cement volume in all samples (8.4% in sample 15 and 4.5% in sample 13). However, the geochemical analysis shows that most cements were precipitated from seawater in a phreatic setting. Van de Plassche (1986) notes that the fast cementation of beachrock can lead to occurrences as high up as the highest astronomical tide (HAT), even if that level is only reached a few times a year. On top of older platforms, as observed at Mission Rocks, cementation is even possible above the HAT, because of a low permeability of the underlying platform, which leads to temporary perched water tables (Van de Plassche 1986).

Our petrographic work has revealed that intraclasts derived from the older calcarenite platform, all possess the same equant, blocky spar, which fills out the entire primary and secondary porosity. Thus, a low permeability of the calcarenite platform is presumable. This is also obvious from numerous puddles that are found on top the platform, which constantly form from spray water accumulating within potholes or similar depressions. Many potholes display a several centimetres-thick layer of salt at the bottom testifying to the fact that the assembled water rather evaporates instead of percolating into the platform`s pore space. Kinsey and Davies (1979) demonstrate that porosity, even in partially cemented beachrocks, reaches only 30% and tends to be lower the longer the beachrock was subaerially exposed. In the case of the well-cemented calcarenite platform, the porosity is expected to be much lower if not completely lost. We consider that the high energy wave regime of Mission Rocks produces a significant amount of spray even during fair weather conditions all year round. It is on these grounds that we interpret this unique composition of cements in these beachrocks to be the result from cementation in marine waters that get trapped on top of the calcarenite platform combined with an occasional influence of meteoric water sapped from the adjoining dunes. These results highlight the importance of understanding facies variability in beachrocks, especially when they are utilised as an indicator of past sea levels. In this case, cementing agent alone cannot be reliably used as an indicator of shoreline occupation.

5.3. Influence on shoreline evolution

Beachrocks, like the one observed at Mission Rocks, have a noticeable influence on shoreline evolution as they act as natural beach defences against coastal erosion (e.g. Chowdhury et al. 1997, Dickinson 1999, Vousdoukas et al. 2007(b)). It is known that beachrocks located in the upper surf and swash zones actively prevent shoreline retreat. At the same time they are subject to constant chemical and mechanical weathering. Coastal erosion is a major concern of global scale, especially in the context of rising global sea level. With this in mind it is not surprising that recent research has focussed on modelling of beach morphodynamics in the presence of beachrocks (e.g. Larson and Kraus 2000, Vousdoukas et al. 2005; 2007(b)). So far, none of these models have considered that rapidly growing, recent beachrocks act as a natural repair-system of, potentially much older, beachrock bodies. Beachrock erosion at Mission Rocks occurs through notch formation and gravitational collapse, surface degradation in the form of potholes or furrows, as well as the development of tensile fractures (Mthembu, pers. comm). The recent beachrock facies that is described in this paper is actively filling and thus repairing sites of focus for chemical and mechanical weathering, especially large joints which act as points of gravitational collapse (cf. Cooper et al. 2019). The infill of fractures and potholes by loose material and subsequent cementation is an ongoing process that slows further deepening. As potholes are a result of mechanical erosion and form due to wave-induced movement of trapped gravel (Russel 1962, Milliman 1974), their formation could come to a complete halt by cementing the gravel onto the platform. Obviously, the erosion of the older beachrock platform is not fully prevented by the facies that is described here. Still, its effect on coastal erosion deserves further attention. It is clear from our results that the high energy setting of the coastline plays an important role in the formation of this beachrock, because it 1) accumulates sediment on top of the platform and 2) provides a significant amount of spray to induce cementation. That way the same wave energy that causes platform erosion in the first place also, counterintuitively, contributes to slowing it down.

6. Conclusions

The main objectives of this study were to document the occurrence of a rare, rapidly forming beachrock at Mission Rocks beach and to interpret it regarding its formation process especially cementation.

Three main conclusions can be summarised from the results:

(1) An unusual beachrock facies forms in a high energy environment on a steep, reflective coastline, and unusually on a pre-existing rocky platform. The formation process is rapid, as at least part of the beachrock must be younger than 1943 as evident from historic remains.

(2) Although situated in the meteoric vadose zone, the precipitation of cement takes place under phreatic conditions and mostly from marine water. This is explained by the effects of constant spray and a low permeability of the underlying platform.

(3) This beachrock facies has a potential effect on the velocity of platform breakdown and thus shoreline evolution.

Commented [US1]: What do we make of the fact that this is a thick veneer and thus didn't require the degree of burial usually needed in the thermodynamics of cement precipitation?

7. Acknowledgements

We wish to express our gratitude to the German Academic Exchange Service (DAAD), who funded this work with a short term scholarship for doctoral candidates, which allowed Miss Falkenroth to travel to South Africa for a two months research stay at UKZN. This study is a contribution to the IGCP Project 639 whose participants receive our thanks for fruitful discussions in the field during the 2nd annual meeting in St Lucia in 2017. The Microscopy and Microanalysis Unit of the UKZN and the University Bonn, namely Mr Rainer Schwartz, are acknowledged for the use of equipment and assistance. Dr Warwick Hastie receives our thanks for providing photographs of the blasting fractures at Mission Rocks, when a pandemic kept us from taking them ourselves. Warwick, JJ Van Den Bergh and Ayanda Mthembu are thanked for a productive and fun fieldtrip.

References

Andreoli, M. A. G., Doucoure, M., Van Bever Donker, J., Brandt, D., Andersen, N. J. B. 1996. Neotectonics of southern Africa – a review. *African Journal of Geoscience*, **3**, 1-16.

Badyukova, Y. N., Svitoch, A. A. 1986. The beach-rock of the Seychelles Islands. *Oceanology*, **26(5)**, 604-608.

Binkley, K. L., Wilkinson, B. H., Owen, R. M. 1980. Vadose beachrock cementation along a Southeastern Michigan marl lake. *Journal of Sedimentary Petrology*, **50**, 953-962.

Bricker, O. P. 1971. Introduction: beachrock and intertidal cement. In: Bricker, O. P. (ed*), Carbonate Cements*. John Hopkins Press, Baltimore, pp. 1-13.

Calvet, F. 1982. Constructive micrite envelope development in vadose continental environment in Pleistocene eoliantes of Mallorca (Spain). *Acta Geologica Hispanica*, **17(3)**, 169-178.

Calvet, F., Cabrera, M. C., Carracedo, J. C., Mangas, J., Pérez-Torrado, F. J., Recio, C., Travé, A. 2003. Beachrocks from the island of La Palma (Canary Islands, Spain). *Marine Geology*, **197**, 75-93.

Cawthra, H., Uken, R. 2012. Modern beachrock formation in Durban, KwaZulu-Natal. *South African Journal of Science*, **108(7/8)**.

Chivas, A., Chappell, J., Polach, H., Pillans, B., Flood, P. 1986. Radiocarbon evidence for the timing and rate of island development, beach-rock formation and hosphatization at Lady Elliot Island, Queensland, Australia. *Marine Geology*, **69**, 273-287.

Chowdhury, S. Q., Fazlul Haq, A. T. M., Hasan, K. 1997. Beachrock in St. Martin`s Island, Bangladesh: Implication of sea level changes on beachrock cementation. *Marine Geology*, **120**, 89-104.

Coetzee, F. 1975. Coastal aeolianites at Black Rock, northern Zululand. *Transactions of the Royal Society of South Africa*, **78**, 313-322.

Cooper, J. A. G. 1991(a). Beachrock formation in low latitudes: implications for coastal evolutionary models. *Marine Geology*, **98**(1), 145-154.

Cooper, J. A. G. 1991(b). Shoreline Changes on the Natal coast: Mkomanzi River mouth to Tugela River mouth. Natal Town & Regional Planning Commission Report 77. The Town & Regional Planning Commission, P/B 9038, Pietermaritzburg, 3200, 57 pp.

Cooper, J. A. G. 2011. Sea Level Studies: Sedimentary indicators of relative sea-level changes – high energy coasts. In: **Elias, S. A.** (ed) *Encyclopedia of Quaternary Science* (2nd edition). Elsevier, 385-395.

Cooper, J. A. G., Green, A. N., Wiles, E. A. 2017. Beachrock morphology and genesis on a paraglacial beach. *Sedimentary Geology*, **360**, 47-53.

Cooper, J. A. G., Green, A. N., Compton, J. S. 2018. Sea-level change in southern Africa since the Last Glacial Maximum. *Quaternary Science Reviews*, **201**, 303-318.

Cooper, J. A. G., Green, A. N., Vital, H., Lima-Filho, F. P. 2019. Geomorphology and clast assemblages of intertidal beachrock: Implications for submerged shoreline preservation. *Geomorphology*, **343**, 106-118.

Davies, P. J., Kinsey, D. W. 1973. Organic and inorganic factors in recent beach rock formation, heron Island, Great Barrier Reef. *Journal of Sedimentary Petrology*, **43**, 59-81.

Deacon, J., Lancaster, N. 1988. *Late Quaternary Palaeo-environments of Southern Africa*. Clarendon Press, Oxford, 225 pp.

Desruelles, S., Fouache, E., Ciner, A., Dalongeville, R., Pavlopoulos, K., Kosun, E., Coquinot, Y., Potdevin, J.-L. 2009. Beachrocks and sea level changes since Middle Holocene: Comparison between the insular group of Mykonos-Delos-Rhenia (Cyclades, Greece) and the southern coast of Turkey. *Global and Planetary Change*, **66(1-2)**, 19-33.

Dickinson, W. R. 1999. Holocene sea-level record on Funafuti and potential impact of global warming on Central Pacific Atolls. *Quaternary Research*, **51**, 124-132.

Easton, W. H. 1974. An unusual inclusion in beachrock. *Journal of Sediment Petrology*, **44**, 693-694.

Falkenroth, M., Schneider, B., Hoffmann, G. 2019. Beachrock as sea-level indicator - A case study along the coastline of Oman (Indian Ocean). *Quaternary Science Reviews*, **206**, 81-98.

Fluegel, E. 2010. *Microfacies of Carbonate Rocks. Analysis, Interpretation and Application* (2nd edition). Springer, 292.

Frankel, E. 1968. Rate of formation of beach rock. *Earth Planetary Science Letters*, **4**, 439-440.

Gaisford, J. 2011. World War Two Flying-boats over Zululand Coast. Natal Society Foundation, *Natalia*, **41**, 34-39.

Ginsburg, R. 1953. Beach rock in South Florida*. Journal of Sedimentary Petrology*, **23**,85-92.

Green, A. N., Goff, J. A., Uken, R. 2007. Geomorphological evidence for upslope canyon-forming processes on the northern KwaZulu-Natal shelf, SW Indian Ocean, South Africa. *Geo-Marine Letters*, **27**, 399-409.

Green, A. N., Cooper, J. A. G., Salzmann, L. 2018. The role of shelf morphology and antecedent setting in the preservation of palaeo-shoreline (beachrock and aeolianite) sequences: the SE African shelf. *Geo-Marine Letters*, **38**(1), 5-18.

Hanor, J. S. 1978. Precipitation of beachrock cements: mixing of marine and meteoric waters vs. CO_2-degassing. *Journal of Sedimentary Petrology*, **48**, 489-501.

Hastie, W. W. 2012. Rock fabric study of the Northern Lebombo and Rooi Rand dyke swarms: regional and local implications. Doctoral dissertation, University of KwaZulu-Natal, Durban, South Africa.

Hayes, M. O. 1979. Barrier island morphology as a function of tidal and wave regime. In: Leatherman, S. (Ed.) *Barrier Island from the Gulf of Mexico*, Academic Press, New York, 3-22.

Hicks, N. 2009. A combined sedimentological-mineralogical study of sediment-hosted gold and uranium mineralization at Danny Dalton, Pongola Supergroup, South Africa. Doctoral dissertation, University of KwaZulu-Natal, Durban, South Africa.

Hillgärtner, H., Dupraz, C., Hug, W. 2001. Microbially induced cementation of carbonate sands: are micritic meniscus cements good indicators of vadose diagenesis? *Sedimentology*, **48**, 117-131.

Hopley, D. 1986. Beachrock as a sea-level indicator. In: **Van de Plassche, O.** (Ed.) *Sea-level research: a manual for the collection and evaluation of data*. Geo Books, Norwich, 157-175.

Kelly, C. S., Green, A. N., Cooper, J. A. G., Wiles, E. 2014. Beachrock facies variability and sea level implications: a preliminary study. *Journal of Coastal Research*, **170**, 736-742.

Kneale, D., Viles, H. A. 2000. Beach cement: incipient $CaCO_3$-cemented beachrock development in the upper intertidal zone, North Uist, Scotland. *Sedimentary Geology*, **132**, 165-170.

Kobluk, D. R., Risk, M. J. 1977. Micritisation and carbonate-grain binding by endolithic algae. *AAPG Bulletin*, **61**, 1069-1082.

Krige, L. J. 1932. The Geology of Durban. *Transactions of the Geological Society of South Africa*, **35**, 37-67.

Larson, M., Kraus, N. C. 2000. Representation of non-erodible (hard) bottoms in beach profile change modelling. *Journal of Coastal Research*, **16** (1), 1-14.

Martin, A. K., Flemming, B. W. 1988. Physiography, structure and geological evolution of the Natal continental shelf. In: **Schumann, E. H.** (ed), *Lecture Notes in Coastal and Estuarine Studies*, 26. Coastal Ocean Studies off Natal, South Africa, 11-46.

Maud, R. R. 1980. The climate and geology of Maputaland. In: **Brunton, M. N., Cooper, K. H.** (eds.) *Studies on the Ecology of Maputaland.* Rhodes University, Grahamstown and the Natal Branch of the Wildlife Society of South Africa, 1-7.

Mauz, B., Vacchi, M., Green, A. N., Hoffmann, G., Cooper, J. A. G. 2015. Beachrock: A tool for reconstructing sea level in the far-field. *Marine Geology*, **362**, 1-16.

McCourt, S., Armstrong, R. A., Grantham, G. H., Thomas, R. J. 2006. Geology and evolution of the Natal belt, South Africa. *Journal of African Earth Sciences*, **46**(1-2), 71-92.

Midgley, D. C., Pitman, W. V., middleton, B. J. 1994. Surface water resources of South Africa 1990; Volume VI Book of Maps, Drainage Regions U, V, W, X, Eastern Escarpment. Water Research Commision.

Milliman, J. D. 1974. *Marine carbonates*. Springer-Verlag, Berlin, 375 pp.

Moes, H., Roussouw, M. 2008. Considerations for the utilization of wave power around South Africa. Workshop on ocean energy. Centre for renewable and Sustainable Energy Studies, Stellenbosh, Abstracts, 36 pp.

Moore, C. H. 1973. Intertidal carbonate cementation in Grand Cayman, West Indies*. Journal of Sedimentary Petrology*, **43**, 591-602.

Neumeier, U. 1999. Experimental modelling of beachrock cementation under microbial influence. *Sedimentary Geology*, **126**, 35-46.

Porat, N., Botha, G. 2008. The luminescence chronology of dune development on the Maputaland coastal plain southeast Africa. *Quaternary Science Reviews*, **27**, 1024-1046.

Ramsay, P. J. 1994. Marine geology of the Sodwana Bay shelf, southeast Africa. *Marine Geology*, **120**, 225-247.

Ramsay, P. J., Cooper, J. A. G. 2002. Late Quaternary Sea-Level Change in South Africa. *Quaternary Research*, **57(1)**, 82-90.

Ramsay, P. J., Mason, T. R. 1990. Development of a type zoning model for Zululand coral reefs, Sodwana Bay, South Africa*. Journal of Coastal Research*, **6**, 829-852.

Rey, D., Rubio, B., Bernabeu, A. M., Vilas, F. 2004. Formation, exposure, and evolution of a high-latitude beachrock in the intertidal zone of the Corrubedo complex (Ria de Arousa, Galicia, NW Spain). *Sedimentary Geology*, **169**, 93-105.

Russel, R. J. 1959. Caribbean beach rock observation*. Zeitschrift der Geomorphologie*, **3**, 227-236.

Russel, R. J. 1962. Origin of beach rock. *Zeitschrift der Geomorphologie*, **6**, 1-16.

Russell, R. J., McIntire, W. G. 1965. Southern hemisphere beach rock. *Geographic Revenue*, **55**, 17-45.

Smith, A. M., Mather, A. A., Bundy, S. C., Cooper, J. A. G. 2010. Contrasting styles of swell-driven coastal erosion: examples from KwaZulu-Natal, South Africa. *Geological Magazine*, **147**, 940-953.

Stoddart, D. R., Cann, J. R. 1965. Nature and origin of beach rock. *Journal of Sedimentary Petrology*, **35**, 243-247.

Tankard, A. J. 1976. Cenozoic sea-level changes, a discussion. *Annals of the South African Museum*,**71**, 1-17.

Vacchi, M., Rovere, A., Zouros, N., Desruelles, S., Caron, V., Firpo, M. 2012. Spatial distribution of sea-level markers on Lesvos Island (NE Aegean Sea): Evidence of differential relative sea-level changes and the neotectonic implications. *Geomorphology*, **159-160**, 50-62.

Vousdoukas, M. I., Velegrakis, A. F., Karambas, T., Valais, G., Zarkoyiannis, S. 2005. Morphodynamics of beachrock-infected beaches: Vatera Beach, NE Mediterranean. In: **Sanchez-Arcilla, A.** (ed.), 5th International Conference on Coastal Dynamics, Barcelona. 12 pp.

Vousdoukas, M. I., Velegrakis, A. F., Plomaritis, T. A. 2007. (a) Beachrock occurence, characteristics, formation mechanisms and impacts. *Earth-Science Reviews*, **85**, 23-46.

Vousdoukas, M. I., Karambas, T. V., Velegrakis, A. F. 2007. (b) Modelling beach profile evolution of beachrock infected beaches, using a Boussinesq model. 32nd Conference of the IAHR, Venice, July, 1-6, 2007. 10 pp.

Wiles, E., Green, A. N., Cooper, J. A. G. 2018. Rapid beachrock cementation on a South African beach: Linking morphodynamics and cement style. *Sedimentary Geology*, **378**, 13-18.

Wright, V. P. 1986. The role of fungal biomineralization in the formation of Early Carboniferous soil fabrics. *Sedimentology*, **33**, 831-838.

Yaltirak, C., Sakinc, M., Aksu, A. E., Hiscott, R. N., Galleb, B., Ulgen, U. B. 2002. Late Pleistocene uplift history along the southwestern Marmara Sea determined from raised coastal deposits and global sea-level variations. *Marine Geology*, **190 (1-2)**, 238-305.

Tables

Outcrop	GPS	Elevation [m a msl]	Sample No.
A	28°17'4.84"S 32°28'58.43"E	1.96	-
B	28°16'57.67"S 32°29'1.39"E	1.08	-
C	28°16'46.37"S 32°29'7.27"E	1.39	-
D	28°16'44.02"S 32°29'8.11"E	1.32	Sample 14
E	28°16'41.47"S 32°29'9.03"E	1.94	Sample 13
F	28°16'34.34"S 32°29'11.97"E	1.8	Sample 15

Table 1: GPS Locations and elevations relative to msl of all occurrences and sampling locations of the unusual beachrock facies.

Sample No.	Cement Style	Share of cement volume [%]
13	Irregular, fibrous rims	41,6
	Pore-filling pseudospar	29,2
	Micrite rims	15,4
	Equant, pore-filling spar	7,9
	Drusy, pore-filling spar	4,5
	Micrite menisci	1,4
14	Isopachous, fibrous rims	34,3
	Micrite rims	24,9
	Pore-filling pseudospar	21,5
	Pore-filling micrite	6,6
	Equant, pore-filling spar	6,1
	Micrite menisci	5,5
	Dog-tooth crust cement	1,1
15	Isopachous, fibrous rims	31,2
	Pore-filling micrite	27,8
	Micrite rims	12,3
	Pore-filling pseudospar	11
	Micrite menisci	8,9
	Drusy, pore-filling spar	8,4
	Equant, pore-filling spar	0,4

Table 2: Bulk volume percentage share of the different cement styles divided by samples

Cement Style	Sample No.	EDX spectra	mol% Mg	Average mol% Mg
Irregular or isopachous, fibrous rims	13	Spectrum 66	19	19
	14	Spectrum 36	25	22
		Spectrum 37	19	
	15	Spectrum 3	16	17,5
		Spectrum 5	17	
		Spectrum 6	21	
		Spectrum 10	20	
		Spectrum 12	20	
		Spectrum 14	11	
		Spectrum 15	18	
Pore-filling pseudospar	13	Spectrum 65	34	34
Micrite rims	14	Spectrum 24	26	27,5
		Spectrum 35	29	
	15	Spectrum 8	77	85,6
		Spectrum 9	97	
		Spectrum 11	83	
Drusy, pore-filling cement	13	Spectrum 44	6	6
		Spectrum 47	6	
		Spectrum 45	17	18,8
		Spectrum 46	17	
		Spectrum 49	21	
		Spectrum 50	18	
		Spectrum 51	19	
		Spectrum 52	21	
	15	Spectrum 16	0	1
		Spectrum 17	1	
		Spectrum 18	2	
		Spectrum 19	1	
Blocky, equant pore-filling spar	13	Spectrum 53	17	15,6
		Spectrum 54	14	
		Spectrum 58	16	
	15	Spectrum 4	1	1

Table 3: Results of the SEM and EDX analysis

Figures

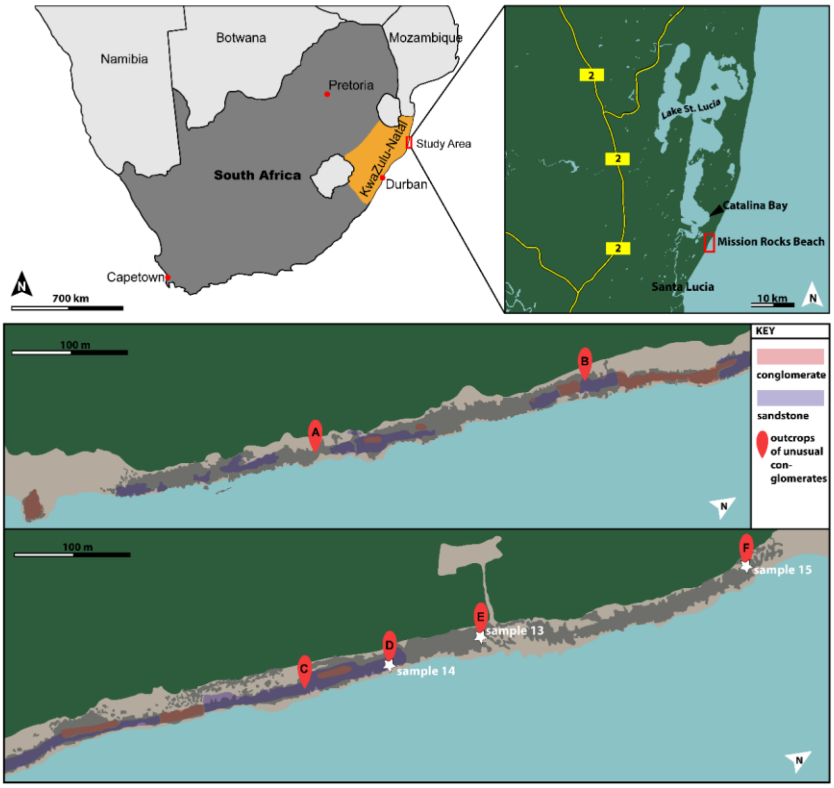

Figure 1: Above: Location of the study area, adjoining Lake St Lucia. Below: Mission Rocks beach and raised platform system. Highlighted are the calcarenite platform lithologies (sandstones and conglomerates) and the occurrences of the fracture filling beachrock facies (A to F) with sampling locations.

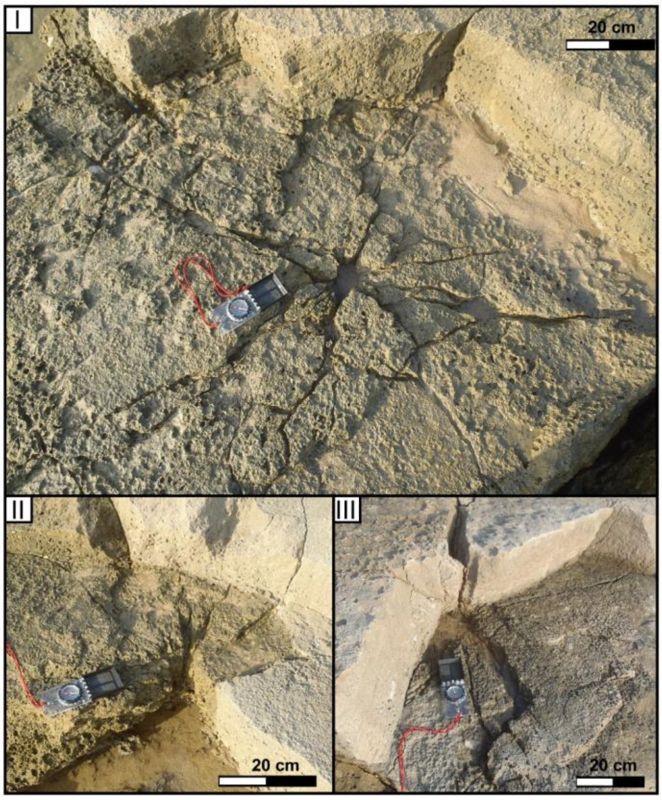

Figure 2: Typical radial blasting fractures within the calcarenite platform at Mission Rocks beach. All pictures were taken near outcrop E (courtesy Dr. Warwick Hastie).

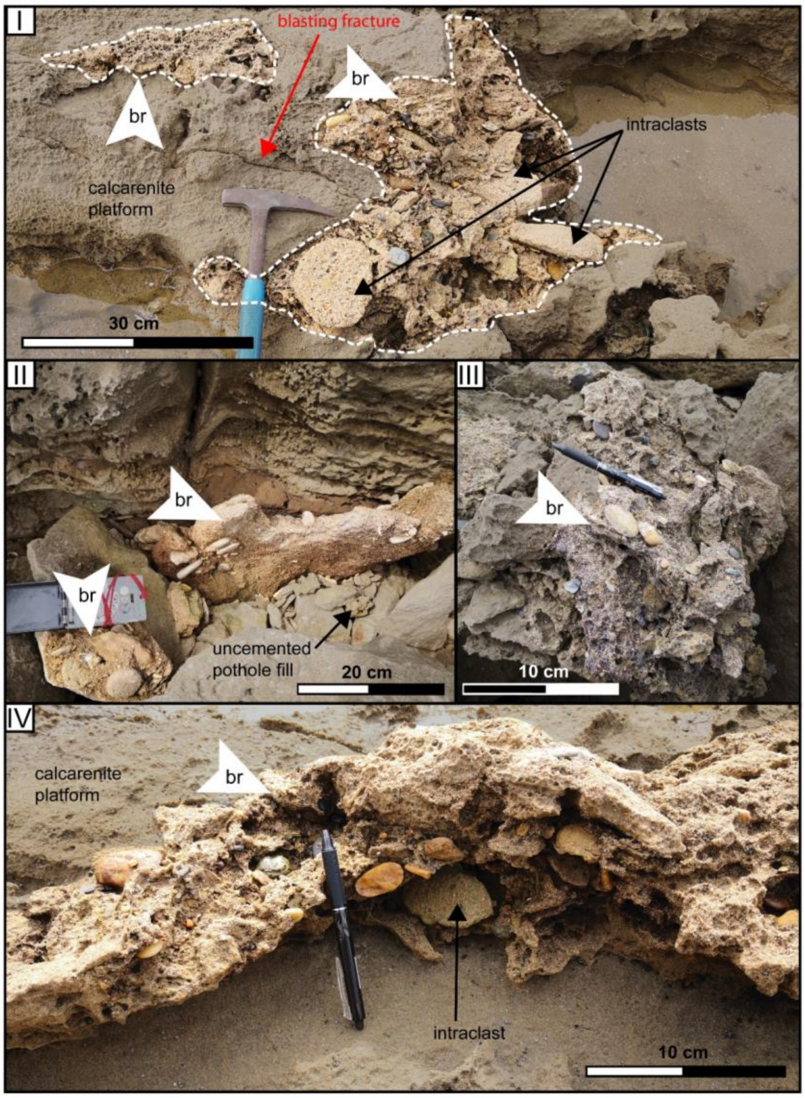

Figure 3: I: A younger beachrock breccia blankets recent blasting fractures atop the older calcarenite platform at outcrop E. The fracture shown here connects to the ones in Figure 2-I. II: The unusual beachrock facies fills a pothole at outcrop D, next to recent, non-cemented gravel. Note that some of the disc-shaped clasts are cemented in an upright position and the beachrock contains a higher percentage of sand-sized material than the non-cemented pothole infill. III: At outcrop F the beachrock contains a high amount of heavy minerals (garnets), which gives its matrix a reddish, purple colour.

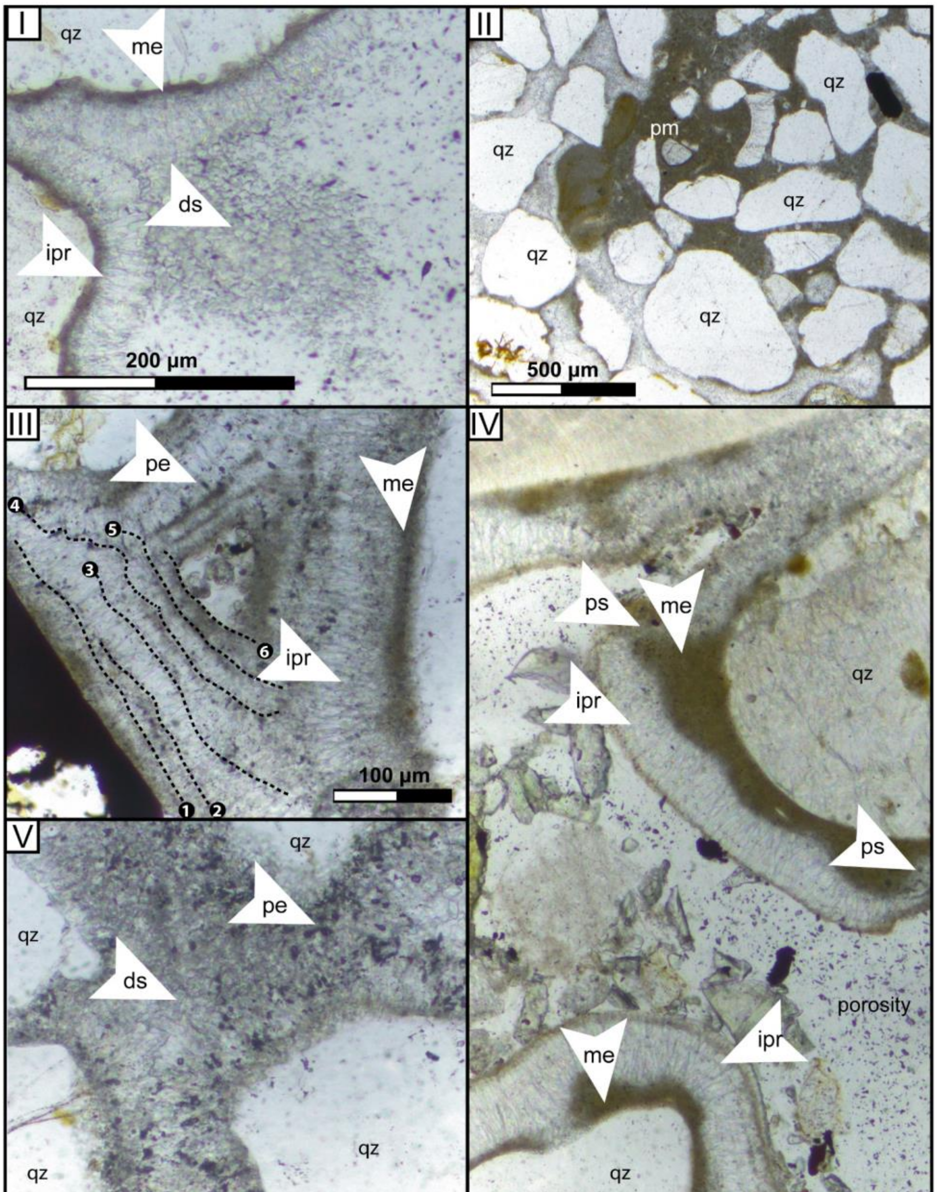

Figure 4: Different styles of cements as observed with a polarising microscope. Ipr: isopachous, prismatic rims; Ds: drusy spar; Pm: pore-filling micrite; Qz: quarz grain; Pe: pseudo peloids; Me: micritic envelope; Ps: pseudospar

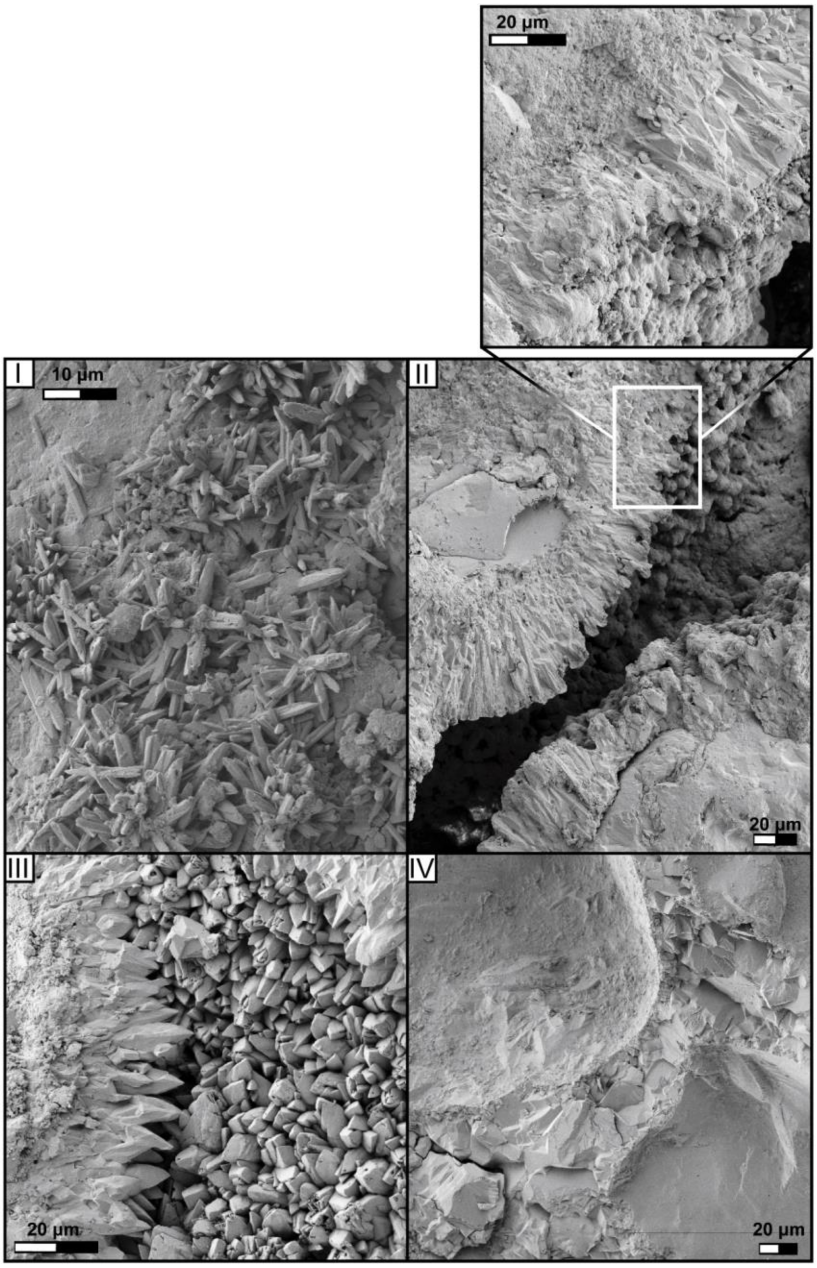

Figure 5: SEM images of samples 13 to 15. I: Small, acicular high-Mg calcite crystals. II: Isopachous, prismatic rims covered by a micritic upbuild (magnification). III: Dog-tooth cement in cross section and as seen from above. IV: Equant, pore-filling spar.

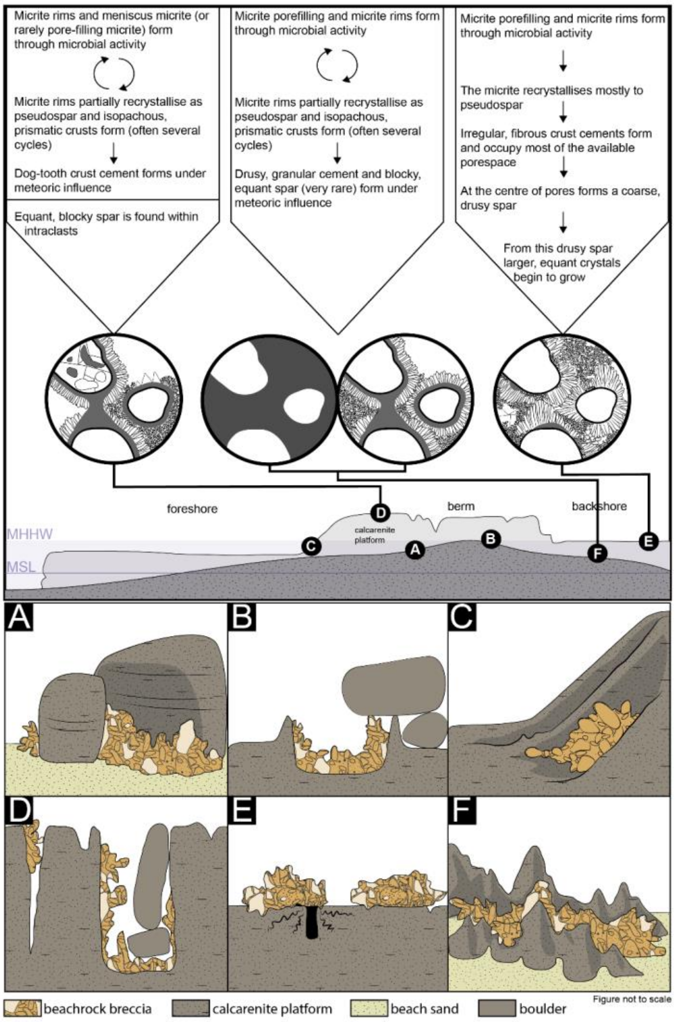

Figure 6: Cementation process of the unusual beachrock facies at Mission Rocks, its position relative to sea level and the spatial relationship of this facies with the underlaying calcarenite platform at locations A to F.

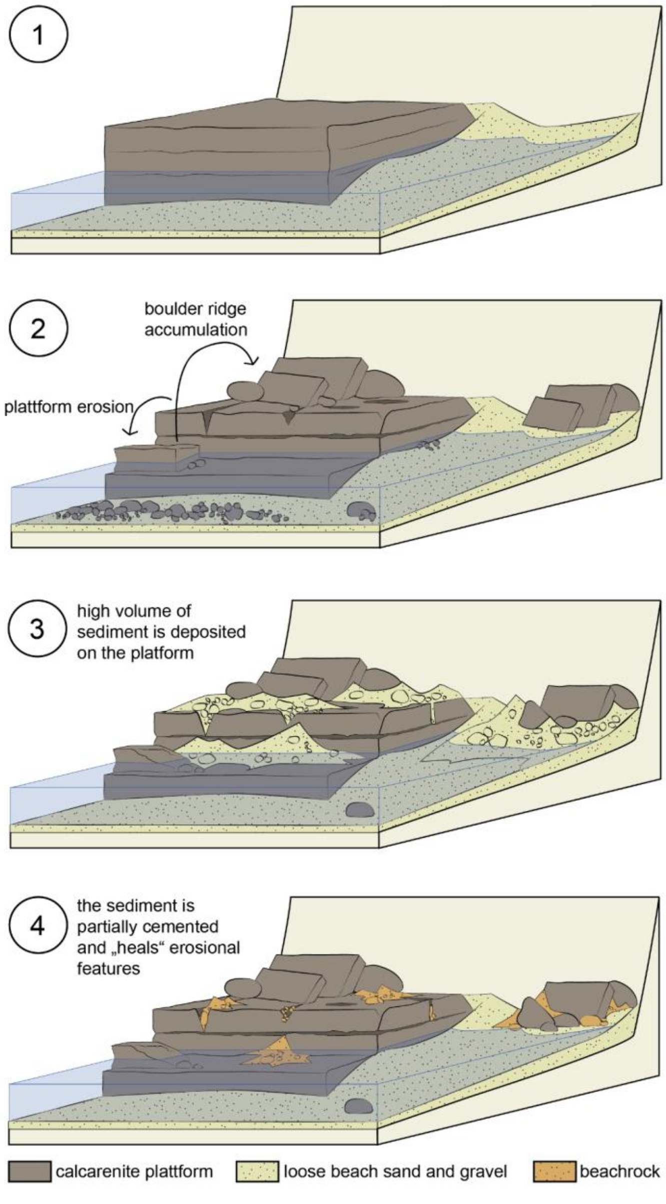

Figure 7: Model of the coastal evolution at Mission Rocks.